Multishell Nanostructures

DOI: 10.1002/ange.201306811

Upconverting Near-Infrared Light through Energy Management in Core–Shell–Shell Nanoparticles**

*Hongli Wen, Hai Zhu, Xian Chen, Tak Fu Hung, Beilei Wang, Guangyu Zhu, Siu Fung Yu, and Feng Wang**

Lanthanide-doped upconversion materials, capable of converting low-density ($<1000\,W\,cm^{-2}$) near-infrared (NIR) excitation to ultraviolet (UV) and visible emissions, have generated a large amount of interests in the areas of information technology, biotechnology, energy, and photonics.[1] Significantly, recent developments in the synthetic and multicolor tuning methods have allowed easy access to upconversion nanoparticles with well-defined phase and size, core–shell structure, optical emission, and surface properties.[2–5] The technological advances provide promising applications in sensitive biodetection and advanced bioimaging without many of the constraints associated with conventional optical biolabels.[6] Despite the attractions, further progress in using upconversion processes has been largely hindered because upconversion nanoparticles are typically sensitized by Yb^{3+} ions that only respond to narrowband NIR excitation centered at 980 nm. The absorption of 980 nm light by the water component in biological samples usually limits deep tissue imaging and induces potential thermal damages to cells and tissues.[7]

Excitation of conventional upconversion nanoparticles at other wavelengths has been proposed to minimize the effect of water absorption.[8] But the use of this technique is limited mainly by the largely sacrificed excitation efficiency. Efforts have also been devoted to tuning the NIR response of photon upconversion through integration of various sensitizers such as metal ions (e.g.; Nd^{3+}, V^{3+} or Cr^{5+}) and organic dyes.[9] The progress has resulted in visible emission by NIR excitation in the 700–900 nm range where the transparency of biological samples is maximal.[9e–h] However, upconversion emission across a broad range of spectra in these systems have not been demonstrated largely owing to the uncontrollable nonradiative processes. Herein, we describe a novel design, based on nanostructural engineering to separate unwanted electronic transitions for constructing a new class of materials displaying tunable upconversion emissions spanning from UV to the visible spectral region by single wavelength excitation at 808 nm. We also show that these nanoparticles can surpass the constraints associated with conventional upconversion nanoparticles for biological studies.

The nanostructure design for management of energy transitions is depicted in Figure 1. A core–shell–shell nanoparticle platform is used to host light-harvesting, upconverting, and optical tuning processes at separate layers through doping of appropriate lanthanide ions. Interlayer energy exchange interactions are mediated by arrays of lanthanide migrator ions that can bridge efficient energy transfer across the core–shell interface while filtering unwanted cross-relaxations. As a result, incompatible optical processes can be rationally combined to achieve flexible and efficient photon energy conversions.

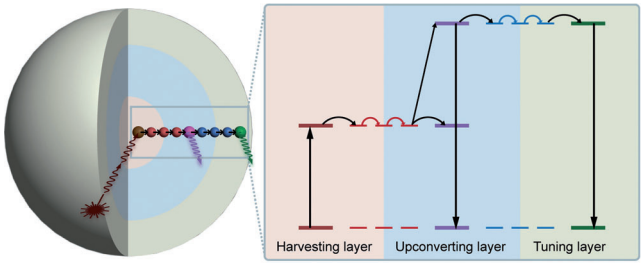

Figure 1. Schematic design of the lanthanide-doped core–shell–shell nanostucture for management of complex energy transitions. Note that core and shell layers are highlighted with different background colors. Photoexcitation takes place in the harvesting layer followed by energy migration to the upconverting layer where low-energy excitation is upconverted into higher-energy emissions. The tuning layer is designed to tune the emission intensity and profile by rejecting surface quenching and by encoding additional emitter ions.

As a proof-of-concept experiment, we employed a $NaYbF_4$@Na(Yb,Gd)F_4@$NaGdF_4$ core–shell–shell nanoparticle host. Nd^{3+} ions featuring several absorption bands in the NIR spectral region were incorporated in the core layer and used to harvest the NIR excitations. The host Yb^{3+} ions are designed to extract the excitation energy from Nd^{3+} and to subsequently transport the energy to the inner shell layer where upconverter ions (Er^{3+}, Ho^{3+} or Tm^{3+}) were confined. $NaGdF_4$ was chosen as the outermost shell layer for protect-

[*] Dr. H. Wen, X. Chen, T. F. Hung, Prof. F. Wang
Department of Physics and Materials Science
City University of Hong Kong
83 Tat Chee Avenue, Hong Kong SAR (China)
E-mail: fwang24@cityu.edu.hk
H. Zhu, Prof. S. F. Yu
Department of Applied Physics
The Hong Kong Polytechnic University
Hong Hum, Hong Kong SAR (China)
B. Wang, Prof. G. Zhu
Department of Biology and Chemistry
City University of Hong Kong
83 Tat Chee Avenue, Hong Kong SAR (China)

[**] This study was supported by CityU through a start-up grant (grant numbers 7200317 and 9610257) and an applied research grant (grant number 9667073) to F.W..

Supporting information for this article is available on the WWW under http://dx.doi.org/10.1002/anie.201306811.

© 2013 Wiley-VCH Verlag GmbH & Co. KGaA, Weinheim

ing the upconverting processes and for tuning the optical emission by encoding additional emitter ions (e.g., Tb^{3+}, Eu^{3+} or Dy^{3+}) that are able to capture the upconverted energy through a network of the Gd sublattice (see Figure S1 in the Supporting Information).

The nanoparticle synthesis was developed using a modified literature procedure[10] and involved the growth of $NaYbF_4$:Nd (50 mol%) core nanoparticles followed by successive deposition of two epitaxial shells of Na(Yb,Gd)F_4:Er^{3+} (or Ho^{3+}, Tm^{3+}) and $NaGdF_4$ (Figure S2). Transmission electron microscopy (TEM) micrographs reveal a rod-like shape of the as-synthesized core–shell–shell nanoparticle (Figure 2a). By contrast, the core nanoparticles

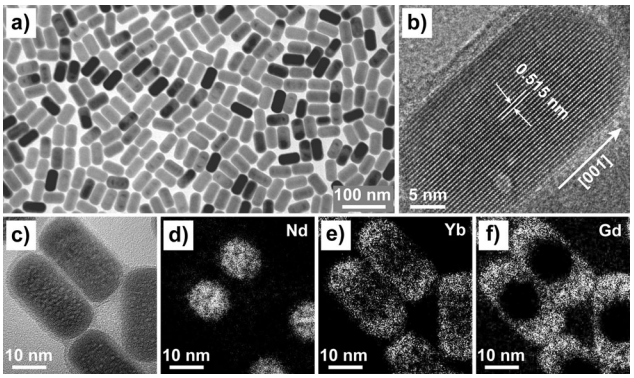

Figure 2. a) Typical TEM image of the as-synthesized $NaYbF_4$:Nd@Na(Yb,Gd)F_4:Er@$NaGdF_4$ core–shell–shell nanoparticles. b) High-resolution TEM image of a nanoparticle shown in (a) reveals a *d*-spacing of 0.515 nm and *c* axis growth direction. c) TEM image of randomly selected nanoparticles for compositional analysis. d–f) Element maps of Nd, Yb, and Gd in the nanoparticles shown in (c).

display a quasi-sphere morphology (Figure S2). The shape evolution phenomena were also observed by several other groups and ascribed to kinetically favored anisotropic shell growth during the coating process.[11] The high-resolution TEM image shows lattice fringes associated with (100) planes (*d*-spacing of 0.515 nm; Figure 2b), indicating that the preferred growth direction is along the *c* axis. The electron energy loss spectroscopy (EELS) analysis illustrates that the elemental distributions of the nanoparticles are very consistent with the designed compositions (Figure 2c–f), confirming the core–shell–shell structure of the nanoparticles.

To evaluate the contribution of Nd^{3+} to the photon upconversion process, we recorded the excitation spectra of $NaYbF_4$@Na(Yb,Gd)F_4:Er@$NaGdF_4$ nanoparticles by monitoring the $^4S_{3/2}\rightarrow{}^4I_{15/2}$ transition of Er^{3+} at 543 nm. As shown in Figure 3a, the nanoparticles without Nd^{3+} dopant display only one excitation band centered at 980 nm, corresponding to $^2F_{7/2}\rightarrow{}^2F_{5/2}$ transition of Yb^{3+}. By contrast, we observed several excitation bands in the range 780–1020 nm for nanoparticles doped with 50 mol% Nd^{3+}. The additional excitation peaks at 798 nm, 808 nm, and 868 nm can be easily assigned to $^4I_{9/2}\rightarrow{}^2H_{9/2}$, $^4I_{9/2}\rightarrow{}^4F_{5/2}$, and $^4I_{9/2}\rightarrow{}^4F_{3/2}$ transitions of Nd^{3+}, respectively. The excitation spectrum clearly supports the Nd-sensitized photon upconversion process. We noticed that a deviation of Nd^{3+} concentration from 50 mol% results in

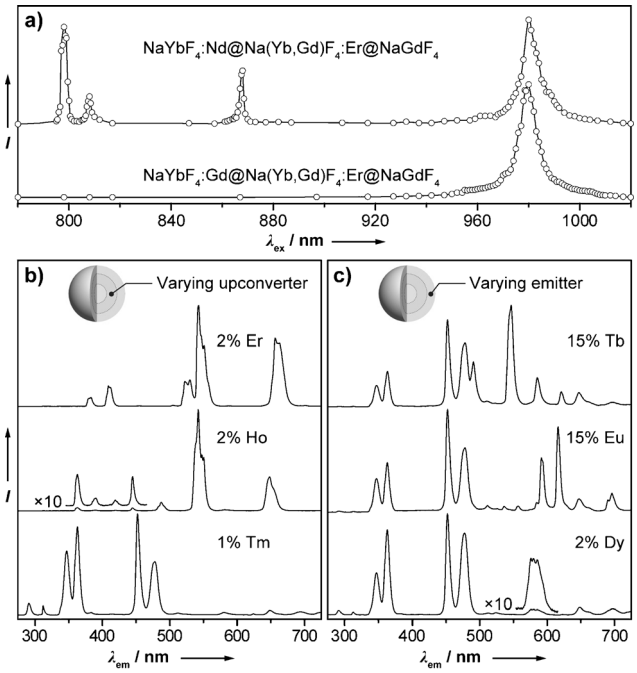

Figure 3. a) Room-temperature excitation spectra of the $NaYbF_4$@Na(Yb,Gd)F_4:Er@$NaGdF_4$ nanoparticles with and without Nd^{3+} dopant. The circlets and solid lines are experimental data and fitting results, respectively. b) Emission spectra of the $NaYbF_4$@Na(Yb,Gd)F_4@$NaGdF_4$ nanoparticles doped with different upconverting ions in the inner shell layer. c) Emission spectra of the $NaYbF_4$@Na(Yb,Gd)F_4@$NaGdF_4$ nanoparticles comprising 1 mol% Tm^{3+} in the inner shell layer and varying emitter ions in the outermost shell layer. The emitter ions produce emission peaks in the visible spectral region by extracting energy from the UV-emitting level of Tm^{3+}.

a drop in the emission intensity of Er^{3+} (Figure S3). The decrease in emission intensity at reduced Nd^{3+} concentrations is consistent with a decrease in the overall absorption of excitation energy. The intensity decline at an elevated Nd^{3+} concentration can be ascribed to enhanced mutual interactions between Nd^{3+} ions that consume the excitation energy.

The nanoparticles comprising different upconverter ions were then investigated by photoluminescence spectroscopy. An 808 nm diode laser that matches the $^4I_{9/2}\rightarrow{}^4F_{5/2}$ transition of Nd^{3+} was used to excite the nanoparticles. The emission spectra in Figure 3b show characteristic emission peaks of Er^{3+}, Ho^{3+}, and Tm^{3+} ranging from UV to the visible spectral region. The appearance of upconversion emission peaks in the UV spectral region is largely owing to the core–shell structure that suppresses deleterious cross-relaxations in the nanoparticles. When the upconverter ions were homogenously doped with Yb^{3+} and Nd^{3+} ions in the core layer, UV upconversion emission peaks essentially disappear and the visible emissions are also largely quenched (Figure S4). Strikingly, for the first time we have realized UV emission of Tm^{3+} at around 300 nm in nanoparticles by 808 nm diode laser excitation through careful control of the dopant concentration of Tm^{3+} (Figure S5). The establishment of population in high-lying energy state of Tm^{3+} also enables further an energy cascade in the Gd sublattice followed by energy trapping by and optical emission from common

© 2013 Wiley-VCH Verlag GmbH & Co. KGaA, Weinheim

lanthanide ions including Tb^{3+}, Eu^{3+}, and Dy^{3+} (Figure 3c). Importantly, the core–shell–shell design allows fine tuning of the upconversion in the shell layers by controlling the dopant concentration according to the previously established protocols (Figure S6).

We next verified the role of the Yb sublattice in the interlayer energy-transfer process by varying the Yb content in the host lattice. As depicted in Figure 4a, a steady decrease

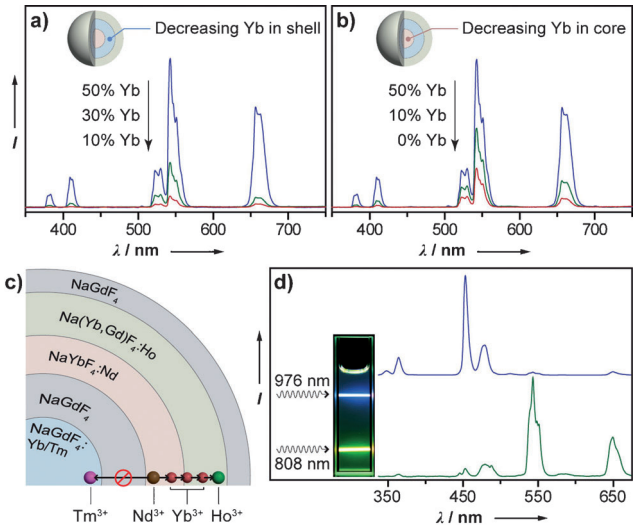

Figure 4. Room-temperature emission spectra of the $NaYbF_4$:Nd@Na(Yb,Gd)F_4:Er@$NaGdF_4$ nanoparticles showing the suppressed Er^{3+} emission at reduced Yb^{3+} concentrations in the a) inner shell and b) core levels. c) Schematic design of tuning the Nd-sensitized upconversion process through nanostructural engineering. d) Emission spectra of the multishelled nanoparticles under excitation at 808 and 976 nm, respectively. Inset: digital camera photograph of corresponding solution sample.

in the upconversion emission intensity was observed when the Yb sublattice in the inner shell layer was diluted with Gd^{3+}. Suppressed upconversion emissions were also observed when Yb^{3+} in the core layer was replaced by optically inert Y^{3+} (Figure 4b). The results confirm that energy hopping through a network of Yb sublattice featuring a short Yb–Yb interionic distance is essential for bridging efficient energy transfer from the Nd^{3+} in the core layer to the upconverting ions in the inner shell layer. The upconversion emission is preserved to some extent when the Yb^{3+} core content was completely exchanged by optically inactive Y^{3+} ions (Figure 4b). The observation is largely ascribed to the high mobility of excitation energy in the core layer associated with a high Nd^{3+} content. Owing to the extensive Nd–Nd interactions, the excitation energy stored in the Nd^{3+} ions can readily arrive at the core–shell interface and be captured by Yb^{3+} ions in the shell layer.

The precise control of interlayer energy transfer through manipulation of the Yb sublattice permits us to deliberately tune the Nd-sensitized upconversion process. The effect was demonstrated by developing novel color kinetic upconversion nanoparticles. For example, we synthesized multishelled nanoparticles comprising dual upconverting ions (Ho^{3+} and Tm^{3+}) at separate layers (Figure 4c). The Ho^{3+} and Nd^{3+} ions were connected by an array of Yb^{3+} ions whereas the Tm^{3+} and Nd^{3+} ions were separated by a $NaGdF_4$ interlayer. On excitation into Nd^{3+} ions at 808 nm, the excitation energy is mainly diverted to Ho^{3+} ions that produce green emissions. In response to 976 nm irradiation, however, Tm^{3+} ions are effectively excited and the blue and UV emissions become prominent. Importantly, the unique optical property is essentially independent of the excitation power density (Figure S7, Supporting Information). By contrast, conventional methods for modulating optical emission of an upconversion nanoparticle generally impose stringent control of the excitation density and suffer from compromised emission intensities.[12]

The nanoparticles capable of upconverting NIR light in the medical spectral window (700–900 nm) offer remarkable advantages over conventional upconversion nanoparticles for biological studies. We transferred the nanoparticles to aqueous solution[13] and assessed the heating effects associated with continuous laser irradiation by using Er^{3+} ions as a thermal probe. The $^2H_{11/2}$ and $^4S_{3/2}$ states of Er^{3+} are thermally coupled and the emission intensity ratio of $^2H_{11/2}\rightarrow{}^4I_{15/2}$ to $^4S_{3/2}\rightarrow{}^4I_{15/2}$ transitions ($R_{H/S}$) provides an accurate probe of surrounding temperature.[14] As shown in Figure 5a,

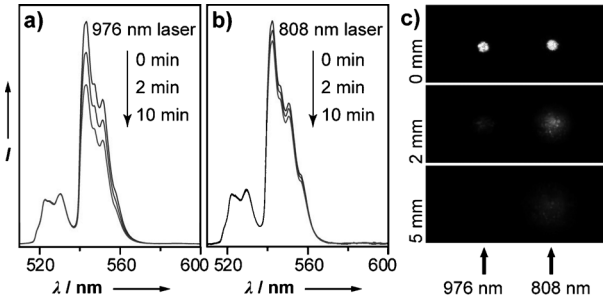

Figure 5. Emission spectra of the surface-modified $NaYbF_4$:Nd@Na(Yb,Gd)F_4:Er@$NaGdF_4$ nanoparticles in aqueous solution after continuous irradiation by diode lasers at a) 976 and b) 808 nm. The spectra were normalized to Er^{3+} emission at 530 nm so that the emission intensities at 543 nm are directly related to the temperature of the solution. c) A comparison of luminescence signal strength of $NaYbF_4$:Nd@Na(Yb,Gd)F_4:Er@$NaGdF_4$ nanoparticles embedded in pork skin tissues of varying thickness by excitation at 976 and 808 nm, respectively.

976 nm excitation induced a quick temperature increase of the nanoparticle solution as indicated by the marked increase in the $R_{H/S}$. By contrast, the $R_{H/S}$ was only marginally altered by 808 nm excitation under the same experimental settings (Figure 5b), suggesting a largely suppressed heating effect. The nanoparticles were also embedded in pork skin tissues of varying thickness and illuminated by 976 nm and 808 nm laser light side by side. By comparing the luminescence signal strength of the nanoparticles at varied distance beneath the tissue surface, 808 nm excitation apparently offered higher sample penetration depth than 976 nm excitation (Figure 5c).

In conclusion, we have demonstrated that core–shell nanostructures can be harnessed to integrate and coordinate several distinct optical processes for realizing unusual upcon-

 © 2013 Wiley-VCH Verlag GmbH & Co. KGaA, Weinheim

version of NIR light in the medical spectral window (about 800 nm) into tunable emissions spanning from UV to the visible spectral region. In addition to providing a platform for enhancing our understanding and control of lanthanide luminescence, these studies also pave the way for constructing novel upconverison nanoparticles that outperform existing biomarkers for therapeutic and diagnostic imaging applications by enabling a better way of excitation.

Received: August 3, 2013
Revised: September 14, 2013
Published online: October 16, 2013

Keywords: core–shell nanoparticles · energy transfer · lanthanides · upconversion

[1] a) F. Auzel, *Chem. Rev.* **2004**, *104*, 139; b) G. Blasse, B. C. Grabmaier, *Luminescent Materials*, Springer, Berlin, **1994**; c) R. Scheps, *Prog. Quantum Electron.* **1996**, *20*, 271; d) B. M. van der Ende, L. Aarts, A. Meijerink, *Phys. Chem. Chem. Phys.* **2009**, *11*, 11081; e) G. Wang, Q. Peng, Y. Li, *Acc. Chem. Res.* **2011**, *44*, 322; f) X. Huang, S. Han, W. Huang, X. Liu, *Chem. Soc. Rev.* **2013**, *42*, 173.

[2] a) H. X. Mai, Y. W. Zhang, R. Si, Z. G. Yan, L. D. Sun, L. P. You, C. H. Yan, *J. Am. Chem. Soc.* **2006**, *128*, 6426; b) J.-C. Boyer, F. Vetrone, L. A. Cuccia, J. A. Capobianco, *J. Am. Chem. Soc.* **2006**, *128*, 7444; c) L. Wang, Y. Li, *Chem. Mater.* **2007**, *19*, 727; d) Z. Li, Y. Zhang, S. Jiang, *Adv. Mater.* **2008**, *20*, 4765; e) F. Wang, Y. Han, C. S. Lim, Y. Lu, J. Wang, J. Xu, H. Chen, C. Zhang, M. Hong, X. Liu, *Nature* **2010**, *463*, 1061; f) D. Chen, Y. Yu, F. Huang, P. Huang, A. Yang, Y. Wang, *J. Am. Chem. Soc.* **2010**, *132*, 9976; g) X. Ye, J. E. Collins, Y. Kang, J. Chen, D. T. N. Chen, A. G. Yodh, C. B. Murray, *Proc. Natl. Acad. Sci. USA* **2010**, *107*, 22430; h) N. J. J. Johnson, W. Oakden, G. J. Stanisz, R. S. Prosser, F. C. J. M. van Veggel, *Chem. Mater.* **2011**, *23*, 3714; i) X. Teng, Y. Zhu, W. Wei, S. Wang, J. Huang, R. Naccache, W. Hu, A. I. Y. Tok, Y. Han, Q. Zhang, Q. Fan, W. Huang, J. A. Capobianco, L. Huang, *J. Am. Chem. Soc.* **2012**, *134*, 8340.

[3] a) G. S. Yi, G. M. Chow, *Chem. Mater.* **2007**, *19*, 341; b) H. X. Mai, Y. W. Zhang, L. D. Sun, C. H. Yan, *J. Phys. Chem. C* **2007**, *111*, 13721; c) H. Schäfer, P. Ptacek, O. Zerzouf, M. Haase, *Adv. Funct. Mater.* **2008**, *18*, 2913; d) H. S. Qian, Y. Zhang, *Langmuir* **2008**, *24*, 12123; e) Y. Liu, D. Tu, H. Zhu, R. Li, W. Luo, X. Chen, *Adv. Mater.* **2010**, *22*, 3266; f) X. Liu, X. Kong, Y. Zhang, L. Tu, Y. Wang, Q. Zeng, C. Li, Z. Shi, H. Zhang, *Chem. Commun.* **2011**, *47*, 11957; g) D. Chen, L. Lei, A. Yang, Z. Wang, Y. Wang, *Chem. Commun.* **2012**, *48*, 5898; h) N. J. J. Johnson, A. Korinek, C. Dong, F. C. J. M. van Veggel, *J. Am. Chem. Soc.* **2012**, *134*, 11068; i) F. Zhang, R. Che, X. Li, C. Yao, J. Yang, D. Shen, P. Hu, W. Li, D. Zhao, *Nano Lett.* **2012**, *12*, 2852; j) J. Shen, G. Chen, T. Y. Ohulchanskyy, S. J. Kesseli, S. Buchholz, Z. Li, P. N. Prasad, G. Han, *Small* **2013**, *9*, 3213.

[4] a) S. Heer, K. Kömpe, H.-U. Güdel, M. Haase, *Adv. Mater.* **2004**, *16*, 2102; b) O. Ehlert, R. Thomann, M. Darbandi, T. Nann, *ACS Nano* **2008**, *2*, 120; c) F. Wang, X. Liu, *J. Am. Chem. Soc.* **2008**, *130*, 5642; d) J. Wang, F. Wang, J. Xu, Y. Wang, Y. Liu, X. Chen, H. Chen, X. Liu, *C. R. Chim.* **2010**, *13*, 731; e) F. Wang, J. Wang, J. Xu, X. Xue, H. Chen, X. Liu, *Spectrosc. Lett.* **2010**, *43*, 400; f) H.-T. Wong, H. L. W. Chan, J. Hao, *Opt. Express* **2010**, *18*, 6123; g) J. Wang, F. Wang, C. Wang, Z. Liu, X. Liu, *Angew. Chem.* **2011**, *123*, 10553; *Angew. Chem. Int. Ed.* **2011**, *50*, 10369; h) G. Tian, Z. Gu, L. Zhou, W. Yin, X. Liu, L. Yan, S. Jin, W. Ren, G. Xing, S. Li, Y. Zhao, *Adv. Mater.* **2012**, *24*, 1226; i) Y. Zhang, J. D. Lin, V. Vijayaragavan, K. K. Bhakoo, T. T. Y. Tan, *Chem. Commun.* **2012**, *48*, 10322; j) G. Chen, H. Qiu, R. Fan, S. Hao, S. Tan, C. Yang, G. Han, *J. Mater. Chem.* **2012**, *22*, 20190; k) E. M. Chan, G. Han, J. D. Goldberg, D. J. Gargas, A. D. Ostrowski, P. J. Schuck, B. E. Cohen, D. J. Milliron, *Nano Lett.* **2012**, *12*, 3839; l) J. Zhao, Z. Lu, Y. Yin, C. McRae, J. A. Piper, J. M. Dawes, D. Jin, E. M. Goldys, *Nanoscale* **2013**, *5*, 944.

[5] a) J. Shen, L. D. Sun, C. H. Yan, *Dalton Trans.* **2008**, 5687; b) F. Wang, X. Liu, *Chem. Soc. Rev.* **2009**, *38*, 976; c) F. Wang, D. Banerjee, Y. Liu, X. Chen, X. Liu, *Analyst* **2010**, *135*, 1839; d) C. Li, J. Lin, *J. Mater. Chem.* **2010**, *20*, 6831; e) J.-C. G. Bünzli, *Chem. Rev.* **2010**, *110*, 2729; f) H. S. Mader, P. Kele, S. M. Saleh, O. S. Wolfbeis, *Curr. Opin. Chem. Biol.* **2010**, *14*, 582; g) J. A. Barreto, W. O'Malley, M. Kubeil, B. Graham, H. Stephan, L. Spiccia, *Adv. Mater.* **2011**, *23*, H18; h) M. Haase, H. Schäfer, *Angew. Chem.* **2011**, *123*, 5928; *Angew. Chem. Int. Ed.* **2011**, *50*, 5808; i) J. Zhou, Z. Liu, F. Li, *Chem. Soc. Rev.* **2012**, *41*, 1323; j) Y. Liu, D. Tu, H. Zhu, X. Chen, *Chem. Soc. Rev.* **2013**, *42*, 6924.

[6] a) S. Wu, G. Han, D. J. Milliron, S. Aloni, V. Altoe, D. V. Talapin, B. E. Cohen, P. J. Schuck, *Proc. Natl. Acad. Sci. USA* **2009**, *106*, 10917; b) M. Wang, C. C. Mi, W. X. Wang, C. H. Liu, Y. F. Wu, Z. R. Xu, C. B. Mao, S. K. Xu, *ACS Nano* **2009**, *3*, 1580; c) S. H. Nam, Y. M. Bae, Y. I. Park, J. H. Kim, H. M. Kim, J. S. Choi, K. T. Lee, T. Hyeon, Y. D. Suh, *Angew. Chem.* **2011**, *123*, 6217; *Angew. Chem. Int. Ed.* **2011**, *50*, 6093; d) Q. Liu, Y. Sun, T. Yang, W. Feng, C. Li, F. Li, *J. Am. Chem. Soc.* **2011**, *133*, 17122; e) J. Jin, Y.-J. Gu, C. W.-Y. Man, J. Cheng, Z. Xu, Y. Zhang, H. Wang, V. H.-Y. Lee, S. H. Cheng, W.-T. Wong, *ACS Nano* **2011**, *5*, 7838; f) H. H. Gorris, R. Ali, S. M. Saleh, O. S. Wolfbeis, *Adv. Mater.* **2011**, *23*, 1652; g) F. Zhang, Q. Shi, Y. Zhang, Y. Shi, K. Ding, D. Zhao, G. D. Stucky, *Adv. Mater.* **2011**, *23*, 3775; h) R. Deng, X. Xie, M. Vendrell, Y.-T. Chang, X. Liu, *J. Am. Chem. Soc.* **2011**, *133*, 20168; i) F. Chen, W. Bu, S. Zhang, X. Liu, J. Liu, H. Xing, Q. Xiao, L. Zhou, W. Peng, L. Wang, J. Shi, *Adv. Funct. Mater.* **2011**, *21*, 4285; j) Y. Yang, Q. Shao, R. Deng, C. Wang, X. Teng, K. Cheng, Z. Cheng, L. Huang, Z. Liu, X. Liu, B. Xing, *Angew. Chem.* **2012**, *124*, 3179; *Angew. Chem. Int. Ed.* **2012**, *51*, 3125; k) C. Wang, L. Cheng, H. Xu, Z. Liu, *Biomaterials* **2012**, *33*, 4872; l) J. Yang, D. Shen, X. Li, W. Li, Y. Fang, Y. Wei, C. Yao, B. Tu, F. Zhang, D. Zhao, *Chem. Eur. J.* **2012**, *18*, 13642; m) N. M. Idris, M. K. Gnanasammandhan, J. Zhang, P. C. Ho, R. Mahendran, Y. Zhang, *Nat. Med.* **2012**, *18*, 1580; n) Y. Zhang, F. Zheng, T. Yang, W. Zhou, Y. Liu, N. Man, L. Zhang, N. Jin, Q. Dou, Y. Zhang, Z. Li, L. P. Wen, *Nat. Mater.* **2012**, *11*, 817; o) L.-L. Li, P. Wu, K. Hwang, Y. Lu, *J. Am. Chem. Soc.* **2013**, *135*, 2411.

[7] a) H. Kobayashi, M. Ogawa, R. Alford, P. L. Choyke, Y. Urano, *Chem. Rev.* **2010**, *110*, 2620; b) Q. Zhan, J. Qian, H. Liang, G. Somesfalean, D. Wang, S. He, Z. Zhang, S. Andersson-Engels, *ACS Nano* **2011**, *5*, 3744; c) X. Xie, X. Liu, *Nat. Mater.* **2012**, *11*, 842.

[8] a) G. Chen, T. Y. Ohulchanskyy, Y. Kachynski, H. Ågren, P. N. Prasad, *ACS Nano* **2011**, *5*, 4981; b) Q. Zhan, S. He, J. Qian, H. Cheng, F. Cai, *Theranostics* **2013**, *3*, 306.

[9] a) J. Qiu, Y. Kawamoto, *J. Appl. Phys.* **2002**, *91*, 954; b) J. Qiu, Y. Kawamoto, J. Zhang, *J. Appl. Phys.* **2002**, *92*, 5163; c) J. F. Suyver, A. Aebischer, D. Biner, P. Gerner, J. Grimm, S. Heer, K. W. Krämer, C. Reinhard, H. U. Güdel, *Opt. Mater.* **2005**, *27*, 1111; d) L. Aboshyan-Sorgho, C. Besnard, P. Pattison, K. R. Kittilstved, A. Aebischer, J.-C. G. Bünzli, A. Hauser, C. Piguet, *Angew. Chem.* **2011**, *123*, 4194; *Angew. Chem. Int. Ed.* **2011**, *50*, 4108; e) W. Zou, C. Visser, J. A. Maduro, M. S. Pshenichnikov, J. C. Hummelen, *Nat. Photonics* **2012**, *6*, 560; f) J. Shen, G. Chen, A.-M. Vu, W. Fan, O. S. Bilsel, C.-C. Chang, G. Han, *Adv. Opt. Mater.* **2013**, *1*, 644; g) Y. F. Wang, G. Y. Liu, L. D. Sun, J. W. Xiao, J. C. Zhou, C. H. Yan, *ACS Nano* **2013**, *7*, 7200; h) X. Xie, N. Gao, R. Deng, Q. Sun, Q. Xu, X. Liu, *J. Am. Chem. Soc.* **2013**, *135*, 12608.

© 2013 Wiley-VCH Verlag GmbH & Co. KGaA, Weinheim

[10] a) F. Wang, J. Wang, X. Liu, *Angew. Chem.* **2010**, *122*, 7618; *Angew. Chem. Int. Ed.* **2010**, *49*, 7456; b) F. Wang, R. Deng, J. Wang, Q. Wang, Y. Han, H. Zhu, X. Chen, X. Liu, *Nat. Mater.* **2011**, *10*, 968; c) Q. Su, S. Han, X. Xie, H. Zhu, H. Chen, C. K. Chen, R. S. Liu, X. Chen, F. Wang, X. Liu, *J. Am. Chem. Soc.* **2012**, *134*, 20849.

[11] a) K. A. Abel, J.-C. Boyer, C. M. Andrei, F. C. J. M. van Veggel, *J. Phys. Chem. Lett.* **2011**, *2*, 185; b) C. Zhang, J. Y. Lee, *ACS Nano* **2013**, *7*, 4393.

[12] J.-C. Boyer, C.-J. Carling, B. D. Gates, N. R. Branda, *J. Am. Chem. Soc.* **2010**, *132*, 15766.

[13] N. Bogdan, F. Vetrone, G. A. Ozin, J. A. Capobianco, *Nano Lett.* **2011**, *11*, 835.

[14] C. D. S. Brites, P. P. Lima, N. J. O. Silva, A. Millán, V. S. Amaral, F. Palacio, L. D. Carlos, *New J. Chem.* **2011**, *35*, 1177.

 © 2013 Wiley-VCH Verlag GmbH & Co. KGaA, Weinheim